

Surface Plasmon Polariton Excitation in Time-modulated Media

T. V. Raziman,^{1,2} Marie Touboul,^{3,4} Riccardo Sapienza,¹ Richard V. Craster,² and Francisco J. Rodríguez-Fortuño^{5,*}

¹*The Blackett Laboratory, Department of Physics,
Imperial College London, London SW7 2AZ, UK*

²*Department of Mathematics, Imperial College London, London SW7 2AZ, UK.*

³*POEMS, CNRS, INRIA, ENSTA, Institut Polytechnique de Paris, 91120 Palaiseau, France*

⁴*Department of Mathematics, UMI 2004 Abraham de Moivre-CNRS,
Imperial College London, London SW7 2AZ, UK.*

⁵*Department of Physics, King's College London, Strand, London WC2R 2LS, UK*

(Dated: July 8, 2025)

Surface plasmon polaritons (SPPs) are central to application areas such as sensing, energy harvesting, and nanoscale optics, and are typically excited via spatial structuring – an approach lacking dynamic control. We demonstrate that step-like time modulation allows the excitation and out-coupling of SPPs through modulating a dispersive Drude-like metal thereby modelling realistic transparent conducting oxides; this establishes a pathway for the active control and extraction of plasmons in experimentally viable time-varying systems. Using finite-difference time-domain simulations we show that time modulation facilitates both the launching and radiation of surface plasmons with frequencies governed by the dispersion of the bounding media. Our results also reveal the generation of time-reflected waves and the emergence of a magnetostatic mode required for matching boundary conditions at the temporal interface.

Modulating material properties in time enables electromagnetic phenomena that are forbidden in static media [1]. Spatially engineered metasurfaces and metamaterials – which have enabled applications such as flat optics, beam shaping, optical computing, and cloaking [2–5] – are constrained by fundamental principles, including energy conservation and reciprocity. Time modulation overcomes these limitations and enables frequency manipulation, non-reciprocal devices, and synthetic super-luminal motion [6–8]. The recent discovery of high-contrast all-optical modulation driven by nonlinearities in transparent conducting oxides (TCOs) has enabled a wide range of optical experiments with propagating waves [9, 10]. However, time modulation of near-field waves remains largely unexplored [11]. The wave equation imbues near fields with unique properties at the expense of sub-wavelength confinement: they overcome fundamental limits [12, 13], exhibit complex three-dimensional polarisations [14], and enhance light-matter interactions at high intensity hotspots [15, 16]. Time modulation of the near field can potentially reveal new applications. Coupling between surface waves and radiation by time modulation has been studied in infinitesimally thin Drude-like current sheets [17], bulk plasmas [18, 19], and waveguides [20].

A notable near-field wave is a surface plasmon polariton (SPP), which is a collective excitation of fields and charges bound to a metal-dielectric interface [21]. SPPs – and plasmons more generally – underpin a wide range of technological applications, including chemical and biological sensing, nanoantennas for quantum emitters, solar energy harvesting, on-chip communication, and photocatalysis [22–26]. The momentum mismatch of SPPs with propagating waves in the surrounding media [Fig. 1(c)] has necessitated the development of var-

ious coupling schemes [21, 27]; however, such spatial schemes are static and limited in their reconfigurability. Structuration in time gives additional freedom and the space-time duality [28] enables the replacement of spatial structuring by time modulation; moreover it lifts the constraint of energy conservation to create new frequencies allowing a propagating wave to couple to a SPP with the same in-plane momentum but now having a different frequency [Fig. 1(c)].

In this Letter, we demonstrate that near-field surface waves can be manipulated and coupled to propagating waves by time modulation of the material properties. In particular, SPPs can be excited and out-coupled at the interface of a dispersive Drude-like metal, by a step-like modulation of the carrier mass. We show that time modulation removes the barrier between propagating waves and the evanescent plasmonic near field, permitting (i) partial out-coupling of surface plasmons into radiated frequencies, and (ii) excitation of a surface plasmon with free-space radiation. Both processes generate time-reflected [29] plasmons and propagating waves, along with a magnetostatic mode in the metal to satisfy boundary conditions. Our results act to motivate experiments and applications by proposing a mechanism to create, manipulate, and extract plasmons in realistic time-modulated systems.

The effect of time modulation on an existing plasmon bound to a metal-dielectric interface is shown in Fig 1(a) by plotting the real magnetic field H_y as a function of space and time; the plasmon lies at the interface between a vacuum ($\epsilon = \epsilon_0$, white) and a Drude metal with plasma frequency ω_{p0} (yellow), with fixed momentum along x (here we chose $k_x = \omega_{p0}/c$). Abruptly increasing the plasma frequency of the metal to $1.5\omega_{p0}$ (blue) at time $t = 0$ modifies the fields and we observe: the plasmon

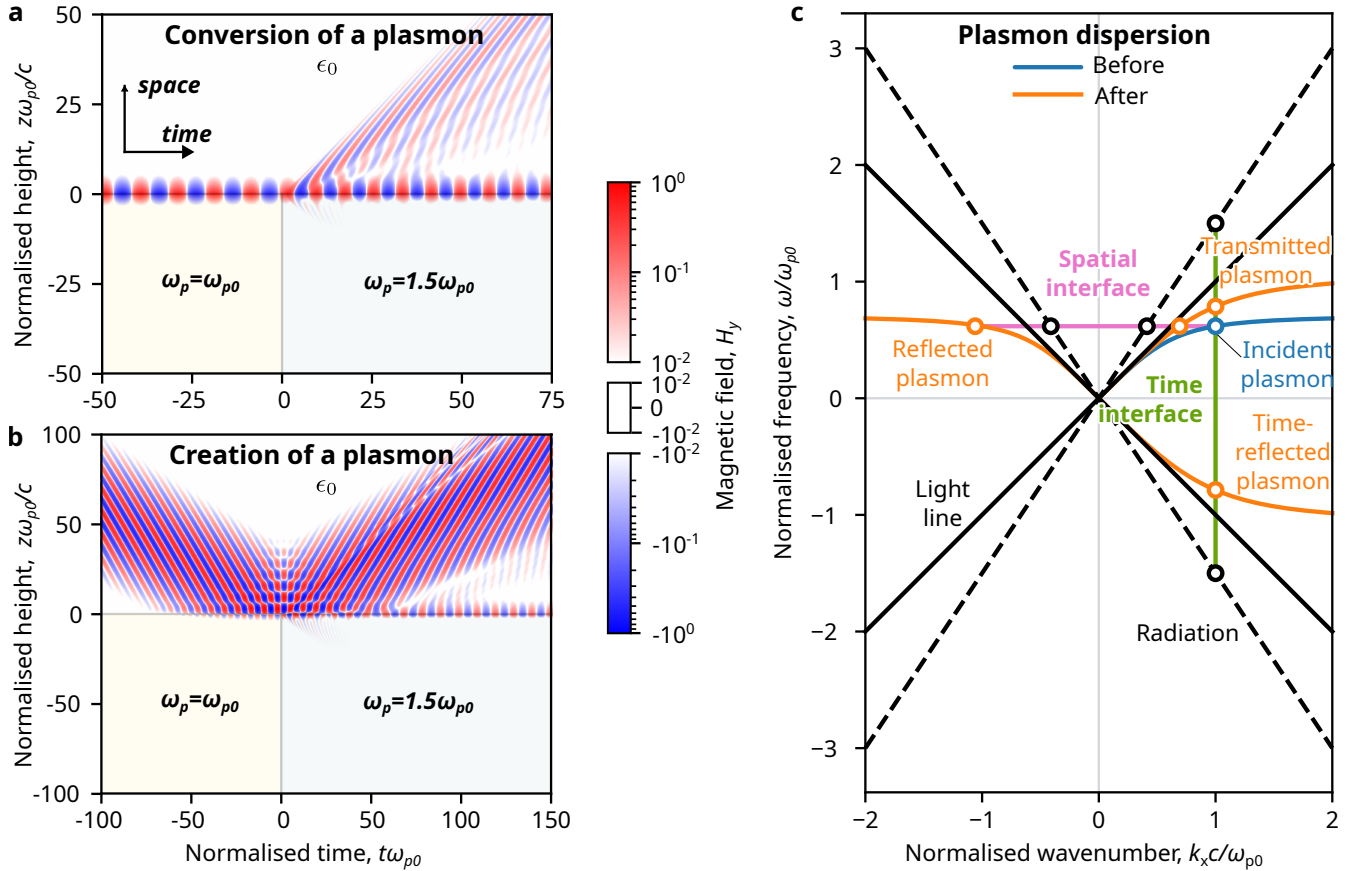


FIG. 1. **Conversion and creation of surface plasmons by time modulation.** (a) A surface plasmon propagates at an interface between a vacuum ($\epsilon = \epsilon_0$, white) and a Drude metal ($\omega_p = \omega_{p0}$, yellow). At $t = 0$, the plasma frequency of the metal is changed suddenly to $1.5\omega_{p0}$ (blue). This changes the frequency of the plasmon and results in plane waves radiating away from the surface. (b) A plane-wave pulse incident from air onto the Drude metal results in the launching of surface plasmons when the plasma frequency is changed abruptly at $t = 0$. (c) Mechanism of launching and outcoupling of plasmons. Conventional manipulation of plasmons relies on spatial structuring compensating for a momentum mismatch (pink). We consider the temporal dual, where a time interface compensates for a frequency mismatch (green).

out-couples partially into radiation after the modulation; the radiation occurs at a range of angles as evident from the phase of the field leaving the interface; after the propagating wave has left, part of the plasmon remains bound to the interface with an increased frequency.

Conversion of the plasmon into radiation suggests that the reciprocal effect of creating a plasmon from propagating light should also be possible. In Fig 1(b) we show this by illuminating a plane wave pulse with fixed momentum ($k_x = 0.7\omega_{p0}/c$) on the same system. The peak of the plane wave pulse falls on the interface at $t = 0$, when the plasma frequency is increased: after the reflected pulse leaves the modulated surface, a plasmon is indeed found at the interface; the reflected pulse is also modified from the original, with clear gaps showing the signature of time modulation.

Figure 2(a) illustrates the conversion of a realistic plasmon with a finite pulse width in more detail (Animation in Supplemental Material [30]). When the plasma fre-

quency of the metal is changed to $1.5\omega_{p0}$ at time $t = 0$, the plasmon stops being a non-reflecting mode, and starts radiating into both half-spaces. The field radiated into air leaves as pulses in forward and backward directions, while the field into the metal decays quickly due to losses. The field that remains bound to the interface splits into three: a part propagating forward, another propagating backwards (time-reflection), and the part fixed near the origin (this ‘frozen mode’, a continuous current and its associated magnetostatic field, is known in bulk plasma time-interfaces [19] and will be discussed later). The animation shows that the bound modes have a frequency higher than that of the original plasmon.

The forward and backward propagating modes bound to the interface are surface plasmons as shown in Fig 2(b); we compute the frequency spectrum of the magnetic field of the fixed-momentum plasmon of Fig. 1(a). The frequency distribution before the modulation is Lorentzian, centered at the analytical SPP frequency (orange dot)

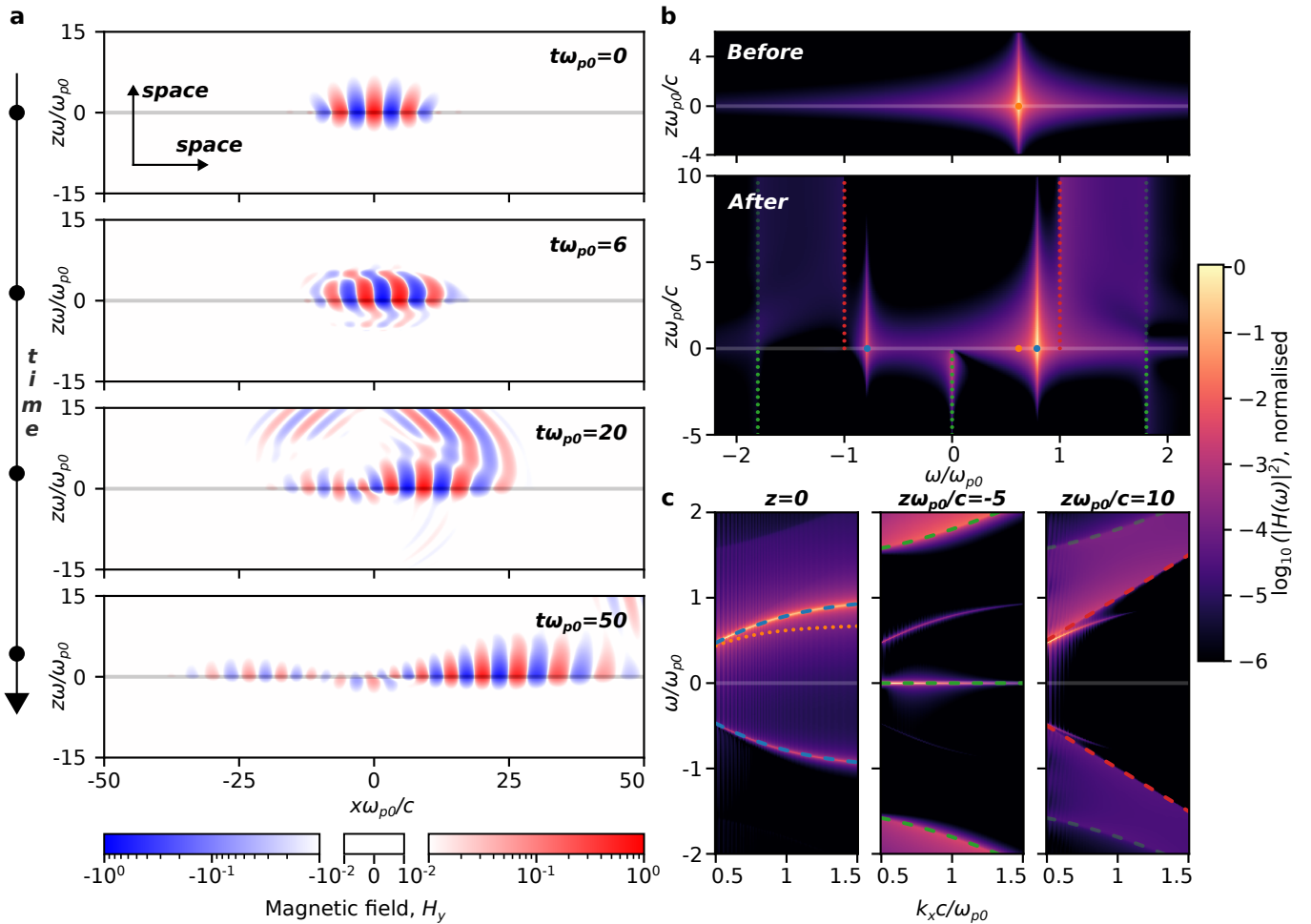


FIG. 2. **Conversion of a surface plasmon by time modulation.** (a) Snapshots of the evolution of the plasmon, starting from modulation at $t = 0$. (b) Normalised intensity of frequency spectrum of the initial and converted magnetic field at different heights. Frequency spectrum is evaluated using a truncated Fourier transform. (c) Dispersion of the converted magnetic field as a function of wavevector of the original plasmon.

and exponentially decaying away from the interface. The most prominent feature after the modulation is the bound wave that retains its shape and shifts to a higher frequency corresponding to the SPP in the modulated medium (blue dot). The bound mode that propagates backwards has the same frequency with a negative sign, confirming that it is a time-reflected plasmon. The frequencies of the radiating field in air range from the light line corresponding to the momentum of the plasmon (red dotted lines) to the dispersion of the bulk metal (green dotted lines). This observation confirms that the out-coupling of radiation is a consequence of the original plasmon ceasing to be a non-reflecting mode after modulation. The field distribution of the old plasmon, which had a single real in-plane momentum k_x and an imaginary k_z , and whose spatial dependence is preserved immediately after the sudden change in plasma frequency, no longer corresponds to a monochromatic eigenmode solution at the interface of air with the new metal plasma frequency.

Instead, the evanescent spatial distribution is decomposed into propagating and evanescent solutions, all with the same k_x (which is a conserved quantity in this problem due to symmetry under spatial translation [31, 32]) but with a range of frequencies, and hence different values of k_z . Some of these out-of-plane momenta are real, corresponding to propagating waves at different angles, and are thus able to transmit to air as radiation. These conclusions are further established by plotting the intensities at, above and below the interface for various values of initial plasmon momentum k_x [Figure 2(c)]. The bound modes and the radiation frequency cutoffs clearly follow the respective dispersion branches.

Finally, we study a propagating Gaussian pulse reflecting from a metal surface that is time-modulated at time $t = 0$ [Figure 3(a). Animation in Supplemental Material [30]]; this pulse contains a spectrum of frequencies and momentum components, due to the temporal and spatial confinement. Until the modulation, the pulse was

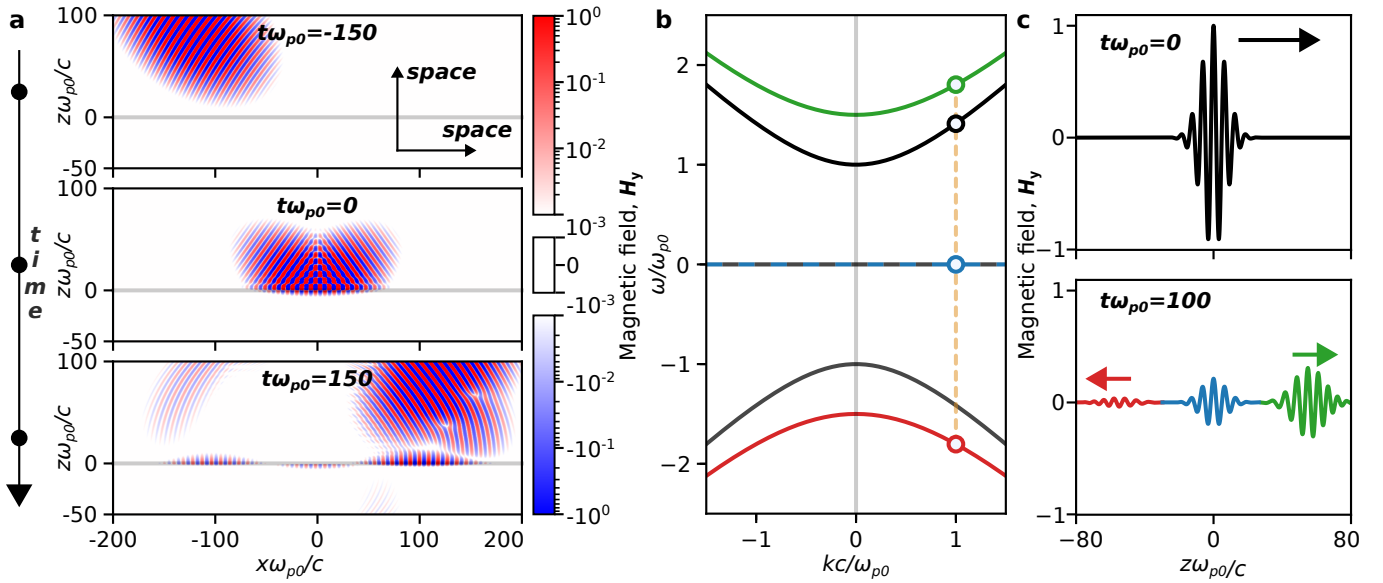


FIG. 3. **Creation of a surface plasmon by time modulation.** (a) Snapshots of a Gaussian pulse incident from air to the metal at $t = 0$, when the plasma frequency is changed. (b) Bulk dispersion curves of the medium. When a medium with a forward-propagating wave (black) undergoes time modulation, it decays into three different branches of the medium: forward-propagating (green), time-reflected (red), and frozen (blue). (c) Magnetic field of the pulse that splits into three.

getting perfectly reflected as if from a mirror. But after the modulation, the reflected pulse is clearly modified. There is also a time-reflected pulse that is reflected in the direction of the incident pulse. After the pulses leave, three bound modes remain on the surface: A forward-propagating plasmon, a time-reflected plasmon, and field that stays fixed to the origin.

We can understand the frozen mode at the origin by studying the bulk dispersion of the metal [Figure 3(b)]. Before modulation, the dispersion of the metal consists of three branches (black lines): two hyperbolas corresponding to forward and backward propagating modes, and a zero frequency mode that is magnetostatic. When the metal is modulated, hyperbolic branches shift (green and red) but the magnetostatic branch (blue) remains. To satisfy boundary conditions of electric and magnetic fields as well as the carrier velocity, the original mode needs to decay into all three of these modes. The zero frequency mode is similar to the magnetostatic field and current that are trapped by a plasma from a propagating field [19]. This phenomenon is also visible in the evolution of a one-dimensional pulse that travels through a bulk metal [Figure 3(c)]. After an abrupt modulation, in addition to the forward and time-reflected waves that propagate in the metal with modified frequency, there is also a wave that stays frozen at the origin. It is the magnetostatic mode that stays at the location of the original pulse while the other branches combine into the new plasmon and the propagating radiation.

In conclusion, we have demonstrated that time modulation can launch surface plasmons and convert them into

propagating waves. The spectral analysis confirms that the excited bound modes correspond to surface plasmon polaritons and the magnetostatic mode of the medium. The ability to create and manipulate SPPs on realistic transparent conducting oxides opens the door to practical experiments and devices based on time-varying media. Although lower frequencies such as the microwave and terahertz regimes do not support SPPs since metals behave as perfect electric conductors, subwavelength structuring can permit “spoof” surface plasmons through an effective Drude-like permittivity [33]. Similar spoof surface waves exist in acoustoelastics in arrays of perfectly rigid bodies [34], and are influenced by space-time modulations [35]. The mechanism studied here could also be leveraged to launch and convert such spoof surface waves across wave domains. Further control may be achieved through periodic temporal or travelling-wave modulation that couples spatial and temporal changes, enabling finer manipulation of plasmon dynamics and improving the efficiency.

Acknowledgments—We acknowledge computational resources and support provided by the Imperial College Research Computing Service (<http://doi.org/10.14469/hpc/2232>). We acknowledge support from the Engineering and Physical Sciences Research Council (EPSRC), grant number EP/Y015673.

* francisco.rodriquez_fortuno@kcl.ac.uk

- [1] E. Galiffi, R. Tirole, S. Yin, H. Li, S. Vezzoli, P. A. Huidobro, M. G. Silveirinha, R. Sapienza, A. Alù, and J. B. Pendry, Photonics of time-varying media, *Advanced Photonics* **4**, 014002 (2022).
- [2] N. Meinzer, W. L. Barnes, and I. R. Hooper, Plasmonic meta-atoms and metasurfaces, *Nature Photonics* **8**, 889 (2014).
- [3] R. C. Devlin, A. Ambrosio, N. A. Rubin, J. P. B. Mueller, and F. Capasso, Arbitrary spin-to-orbital angular momentum conversion of light, *Science* **358**, 896 (2017).
- [4] H. Zheng, Q. Liu, I. I. Kravchenko, X. Zhang, Y. Huo, and J. G. Valentine, Multichannel meta-imagers for accelerating machine vision, *Nature Nanotechnology* **19**, 471 (2024).
- [5] X. Ni, Z. J. Wong, M. Mrejen, Y. Wang, and X. Zhang, An ultrathin invisibility skin cloak for visible light, *Science* **349**, 1310 (2015).
- [6] Y. Zhou, M. Z. Alam, M. Karimi, J. Upham, O. Reshef, C. Liu, A. E. Willner, and R. W. Boyd, Broadband frequency translation through time refraction in an epsilon-near-zero material, *Nature Communications* **11**, 2180 (2020).
- [7] X. Guo, Y. Ding, Y. Duan, and X. Ni, Nonreciprocal metasurface with space-time phase modulation, *Light: Science & Applications* **8**, 123 (2019).
- [8] A. C. Harwood, S. Vezzoli, T. V. Raziman, C. Hooper, R. Tirole, F. Wu, S. A. Maier, J. B. Pendry, S. A. R. Horsley, and R. Sapienza, Space-time optical diffraction from synthetic motion, *Nature Communications* **16**, 5147 (2025).
- [9] M. Z. Alam, I. De Leon, and R. W. Boyd, Large optical nonlinearity of indium tin oxide in its epsilon-near-zero region, *Science* **352**, 795 (2016).
- [10] W. Jaffray, S. Saha, V. M. Shalaev, A. Boltasseva, and M. Ferrera, Transparent conducting oxides: from all-dielectric plasmonics to a new paradigm in integrated photonics, *Advances in Optics and Photonics* **14**, 148 (2022).
- [11] A. C. Valero, S. Gladyshev, D. Globosits, S. Rotter, E. A. Muljarov, and T. Weiss, Resonant states of structured photonic time crystals (2025).
- [12] G. T. Papadakis, M. Orenstein, E. Yablonovitch, and S. Fan, Thermodynamics of Light Management in Near-Field Thermophotovoltaics, *Physical Review Applied* **16**, 064063 (2021).
- [13] J. B. Pendry, Negative Refraction Makes a Perfect Lens, *Physical Review Letters* **85**, 3966 (2000).
- [14] J. S. Eismann, L. H. Nicholls, D. J. Roth, M. A. Alonso, P. Banzer, F. J. Rodríguez-Fortuño, A. V. Zayats, F. Nori, and K. Y. Bliokh, Transverse spinning of unpolarized light, *Nature Photonics* **15**, 156 (2021).
- [15] L. H. Nicholls, F. J. Rodríguez-Fortuño, M. E. Nasir, R. M. Córdova-Castro, N. Olivier, G. A. Wurtz, and A. V. Zayats, Ultrafast synthesis and switching of light polarization in nonlinear anisotropic metamaterials, *Nature Photonics* **11**, 628 (2017).
- [16] W. A. Challener, C. Peng, A. V. Itagi, D. Karns, W. Peng, Y. Peng, X. Yang, X. Zhu, N. J. Gokemeijer, Y.-T. Hsia, G. Ju, R. E. Rottmayer, M. A. Seigler, and E. C. Gage, Heat-assisted magnetic recording by a near-field transducer with efficient optical energy transfer, *Nature Photonics* **3**, 220 (2009).
- [17] E. Galiffi, Y.-T. Wang, Z. Lim, J. Pendry, A. Alù, and P. A. Huidobro, Wood Anomalies and Surface-Wave Excitation with a Time Grating, *Physical Review Letters* **125**, 127403 (2020).
- [18] M. I. Bakunov and S. N. Zhukov, Conversion of a surface electromagnetic wave at the boundary of a time-varying plasma, *Plasma Physics Reports* **22**, 649 (1996).
- [19] M. I. Bakunov and S. N. Zhukov, Trapping of an electromagnetic wave by the boundary of created plasma, *Journal of Experimental and Theoretical Physics* **86**, 696 (1998).
- [20] A. Shlivinski and Y. Hadad, Universal transient radiation dynamics by abrupt and soft temporal transitions in optical waveguides, *Nanophotonics* **14**, 785 (2025).
- [21] S. A. Maier, *Plasmonics: Fundamentals and Applications* (Springer US, New York, NY, 2007).
- [22] K. A. Willets and R. P. V. Duyne, Localized Surface Plasmon Resonance Spectroscopy and Sensing, *Annual Review of Physical Chemistry* **58**, 267 (2007).
- [23] S. Kühn, U. Håkanson, L. Rogobete, and V. Sandoghdar, Enhancement of Single-Molecule Fluorescence Using a Gold Nanoparticle as an Optical Nanoantenna, *Physical Review Letters* **97**, 017402 (2006).
- [24] K. R. Catchpole and A. Polman, Plasmonic solar cells, *Optics Express* **16**, 21793 (2008).
- [25] J. T. Kim, J. J. Ju, S. Park, M.-S. Kim, S. K. Park, and M.-H. Lee, Chip-to-chip optical interconnect using gold long-range surface plasmon polariton waveguides, *Optics Express* **16**, 13133 (2008).
- [26] M. Thangamuthu, T. V. Raziman, O. J. F. Martin, and J. Tang, Review—Origin and Promotional Effects of Plasmonics in Photocatalysis, *Journal of The Electrochemical Society* **169**, 036512 (2022).
- [27] M. Aftab, M. S. Mansha, T. Iqbal, and M. Farooq, Surface Plasmon Excitation: Theory, Configurations, and Applications, *Plasmonics* **19**, 1701 (2024).
- [28] G. P. Agrawal, Space-Time Duality in Optics: Its Origin and Applications, *Photonics* **12**, 611 (2025).
- [29] J. T. Mendonça and P. K. Shukla, Time Refraction and Time Reflection: Two Basic Concepts, *Physica Scripta* **65**, 160 (2002).
- [30] See Supplemental Material at [URL will be inserted by publisher] for animations of wave evolution due to time modulation.
- [31] I. Liberal, A. Ganfornina-Andrades, and J. E. Vázquez-Lozano, Spatiotemporal Symmetries and Energy-Momentum Conservation in Uniform Spacetime Metamaterials, *ACS Photonics* **11**, 5273 (2024).
- [32] J. Zhang, W. Donaldson, and G. P. Agrawal, Conservation law for electromagnetic fields in a space-time-varying medium and its implications, *Physical Review A* **110**, 043526 (2024).
- [33] J. B. Pendry, L. Martín-Moreno, and F. J. Garcia-Vidal, Mimicking surface plasmons with structured surfaces, *Science* **305**, 847 (2004).
- [34] J. Christensen, Z. Liang, and M. Willatzen, Minimal model for spoof acoustoelastic surface states, *AIP Advances* **4**, 124301 (2014).
- [35] K. Pham and A. Maurel, How space-time modulations modify spoof surface plasmons and scattering properties in acoustic metagratings, *Physical Review B* **108**, 024303 (2023).
- [36] A. Bahrami, K. D. Kinder, Z. Li, and C. Caloz, Space-time wedges, *Nanophotonics* 10.1515/nanoph-2024-0526 (2025).

Appendix: Theoretical model—We consider transverse magnetic (TM) polarised waves with magnetic field $H_y\hat{\mathbf{y}}$, with the interface between air ($z \geq 0$) and the metal ($z \leq 0$) as the xy -plane. The electric field is given by $E_x\hat{\mathbf{x}} + E_z\hat{\mathbf{z}}$. Assuming an $\exp(ik_x x)$ dependence for all fields, we have the Maxwell's equations in air,

$$-\mu_0 \frac{\partial H_y}{\partial t} = \frac{\partial E_x}{\partial z} - ik_x E_z, \quad (\text{A1})$$

$$\epsilon_0 \frac{\partial E_x}{\partial t} = -\frac{\partial H_y}{\partial z}, \quad (\text{A2})$$

$$\epsilon_0 \frac{\partial E_z}{\partial t} = ik_x H_y. \quad (\text{A3})$$

We treat the metal as a Drude medium, made of charges with mass m , charge q and number density N , moving with speed $v_x\hat{\mathbf{x}} + v_z\hat{\mathbf{z}}$ and decaying with decay constant γ . The Maxwell's equations for the time evolution of the electric field in the metal become

$$\epsilon_0 \frac{\partial E_x}{\partial t} = -Nqv_x - \frac{\partial H_y}{\partial z}, \quad (\text{A4})$$

$$\epsilon_0 \frac{\partial E_z}{\partial t} = -Nqv_z + ik_x H_y, \quad (\text{A5})$$

while the equation of motion of the charges is given by

$$\frac{\partial v_i}{\partial t} = -\gamma v_i + \frac{qE_i}{m}, \quad (\text{A6})$$

for $i = x, z$. This results in a dispersive permittivity for the metal,

$$\epsilon(\omega) = 1 - \frac{\omega_p^2}{\omega^2 + i\gamma\omega}, \quad (\text{A7})$$

where the plasma frequency ω_p is given by

$$\omega_p^2 = \frac{Nq^2}{m\epsilon_0}. \quad (\text{A8})$$

We assume that the modulation changes only the mass $m(t)$, thereby modifying the plasma frequency $\omega_p(t)$. Integrating the differential equations across the spatial and temporal interfaces, we obtain that the fields

H_y, E_x, E_z, v_x and v_z are continuous across the temporal interface, whereas H_y and E_x are continuous across the spatial interface. This treatment avoids issues with matching boundary conditions at the spacetime corner [36], as the spatial and temporal boundary conditions are directly compatible.

Finite difference time domain simulations—We use finite difference time domain (FDTD) simulations to study the evolution of the fields under time modulation. Due to the $\exp(ik_x x)$ form for the fields and invariance along y , we can set up the FDTD system as one-dimensional in space along z . We evaluate the fields H_y, E_x, E_z (and v_x, v_z in the metal) on a co-located grid. We compute spatial gradients using central differences, and use a fourth order Runge-Kutta method to evolve the fields in time. Choosing the vertical extents of the media large enough avoids reflections within the simulation time.

The ideal plasmon in Fig. 1(a) has a fixed in-plane momentum $k_x = k_0 = \omega_{p0}/c$ and can be directly simulated in this fashion. The plasmon pulse in Fig. 2 has a finite width in space and thus in momentum. We computed it by performing 1-D FDTD simulations of multiple ideal plasmons at momenta separated by $dk_x = 0.01k_0$ and integrating them with weights given by a Gaussian of width $0.3k_0$.

The plane wave pulse in Fig. 1(b) has a fixed in-plane momentum $k_x = 0.7k_0$, allowing a single FDTD simulation to model its evolution. The pulse is composed of plane waves with a Gaussian distribution of vertical momenta k_z centered around $0.5k_0$ and width of $0.1k_0$. The realistic Gaussian pulse in Fig. 3 is computed in a similar fashion as the realistic plasmon, by performing 1-D FDTD simulations of multiple pulses with different fixed in-plane momenta and integrating them with Gaussian weights.

Spectra—We compute the spectra $H_y(z, \omega)$ in Fig. 2(b,c) as a function of height and frequency by performing a temporal Fourier transform of the magnetic field $H_y(z, t)$ computed by FDTD simulations. As the plasmon decays in time, its fields diverge at $t = -\infty$. We hence perform the Fourier transform only for $t \geq 0$, allowing us to consider only the fields after the modulation. We ensure that the fields have decayed sufficiently at the end of the simulation period so that the Fourier integral has converged.